

Spherical Laser Point Sampling with Application to 3D Scene Genetic Registration

Jorge L. Martínez, Antonio Reina and Anthony Mandow

Dep. Ingeniería de Sistemas y Automática, E.T.S. Ingenieros Industriales
Universidad de Málaga, Plaza El Ejido s/n, 29013 Málaga, Spain
Email: jlmartinez@uma.es, Tel: (+34) 952 131408, Fax: (+34) 952 131413

Abstract—Scene registration of 3D laser rangefinder scans is increasingly being required in applications, such as mobile robotics, that demand a timely response. For speeding up point matching methods, the large amount of range data should be reduced. This sampling, in turn, can have a significant impact on accuracy. In particular, Genetic Algorithms provide a robust optimization method that avoids local minima for scan matching, but their computational cost grows with the number of points. This paper proposes a new point sampling strategy that considers the spherical scanning process of most sensors to equalize the measure-direction density. This fast sampling method reduces the number of points without loss of relevant scene information. It is experimentally compared with other systematic approaches for the case of actual scene genetic registration.

I. INTRODUCTION

Scan registration can be defined as finding the translation and rotation of a projected scan contour that produces maximum overlap with a reference scan or a previous model. Scan matching is a highly non-linear problem with no analytical solution that requires an initial estimation to be solved iteratively. In addition, some applications of registration with 3D laser range-finders, like mobile robotics [1], impose time constraints to this problem, in spite of the large amount of raw data to be processed.

Registration of 3D scenes from laser range data is more complex than matching 2D views:

- The amount of raw data is substantially bigger.
- The number of degrees of freedom increases twofold.

Moreover, registration of scenes is different from modeling single objects in several aspects:

- The scene can have more occlusions and more invalid ranges.
- The scene may contain points from unconnected regions.
- All scan directions in the scene may contain relevant information.

There are two general approaches for 3D scan registration: feature matching and point matching. The goal of feature matching is to find correspondences between singular points, edges or surfaces from range images [2]. The segmentation process used to extract and select image primitives determines computation time and maximum accuracy.

On the other hand, point matching techniques try to directly establish correspondences between spatial points from two views. Exact point correspondence from different scans is impossible due to a number of facts: spurious ranges, random noise, mixed pixels, occluded areas and discrete angular resolution. This is why point matching is usually regarded as an optimization problem, where the maximum expected precision is intrinsically limited by the working environment and by the rangefinder performance.

Different optimization techniques have been proposed for point matching methods. They have an important computational cost, which depends mainly on the number of points. Local search methods, such as Iterative Closest Point (ICP) [3] [4] and its many variants [5] or the gradient-based Levenberg-Marquardt method [6] provide faster convergence, but they can get stuck in local minima. This problem is avoided with the use of Simulated Annealing [7] or Genetic Algorithms (GA) [8], which introduce a stochastic component in the search, at the cost of even more expensive computation. Furthermore, hybrid approaches combine GA estimation with faster local refinements based on ICP [9] or hill-climbing [10].

The most straightforward approach to improve computation time for point matching is to reduce the number of points to be matched. However, this can have a great impact on matching accuracy. This sampling process usually has to be applied only once for each scan registration.

Several point sampling methods have been proposed:

- No sampling at all [3]. This is the case for 2D scan matching due to the low number of points [8] [9].
- Random sampling from raw data [11] [12].
- Uniform sampling uses equally distributed data from the scan stream [4].
- Reduction filter, where multiple close points of the same 2D scan slice are averaged into one [1].
- Mesh sampling selects vertices based on a spatial subdivision of the point cloud [13].
- Normal-space sampling selects surface points whose normal vectors are distributed uniformly in all directions [5].
- Selection of points with higher image gradients in laser reflectance measurements [14].

Randomized and uniform sampling are systematic meth-

ods independent of actual range values. Reduction filter, mesh, normal-space, and image gradient methods require processing of laser readings.

This work proposes a new systematic point sampling method that equalizes measure-direction density based on the spherical nature of data of most 3D scanners. This method can be applied to reduce computational cost of optimization-based registration techniques, and has been employed to improve efficiency of time-expensive GA matching.

The paper is organized as follows. Next section surveys the use of GA for scan registration. Section III proposes the new spherical sampling method. Then, the experimental setup is described and the experimental comparison between systematic point sampling methods is reported. Finally, some conclusions and future work are presented in section V.

II. SCAN MATCHING WITH GENETIC ALGORITHMS

GAs, sometimes referred to as evolutionary programming, run a tournament between a population of possible solutions that mimics natural selection. They provide a derivative-free stochastic optimization tool, where each point in a solution space is encoded into a bit string (chromosome) and is associated with a fitness value according to a cost function. Starting from an initial random population, points with better fitness values are used to construct a new population of solutions by means of genetic operators. Basically, these are:

- selection, that determines which individuals survive to the next generation,
- crossover, that generates new chromosomes by randomly combining parts from good solutions, and
- mutation, that sporadically changes some bits of the new individuals.

Thus, after several iterations (generations), the overall fitness value is improved by exploiting the best solutions and exploring new possibilities.

The application of GAs to scan registration can be classified into two groups, depending on the meaning of the genes:

- Correspondence-based encoding: for each projected point, a gene contains an index that identifies the corresponding point in the reference scan [8] [11] [12]. This chromosome (set of matched points) leads to the calculation of a unique least-squares-error transformation between both views.
- Pose-based encoding: each gene represents a degree of freedom. Thus, the chromosome is composed of 3 genes (2 translational and 1 rotational displacements) for 2D problems [9], and of 6 genes (3 translational and 3 rotational displacements) for 3D views [15] [10]. Points can be projected from one scan to another according to the transformation.

The problem with the first strategy is that, even with a low number of points to be projected, the size of chromosomes can be excessively large, and, consequently, the search space too vast. Thus, it has been applied to 2D registration [8] or simple 3D object surface matching [11] [12]. Point reduction can be applied both to the projected (limiting the number of

genes of a chromosome) and reference scans (reducing the number of bits of a gene).

For the second strategy, point correspondence for every chromosome is computationally expensive. Besides, not only accuracy grows with the number of bits employed to represent each gene, but also the search space. Data reduction is applied to the projected scan only, since the complete reference scan is needed to search for precise correspondences.

As for the fitness function to be optimized by the GA, two different types have been employed:

- Object surface properties such as normal vectors [11] or interpenetration measure [10].
- Distances between matched points, either Euclidean [8] [15] [12] or in polar ranges [9]. Unmatchable points are usually discarded from the fitness function by applying a certain threshold.

In any case, the major drawback of GAs for scan matching is their computational load. Exploiting parallelism of the GA is one possibility to solve this problem from a hardware standpoint [15]. However, the most straightforward approach is algorithmic reduction of the number of points to be projected (i.e., point sampling) [10].

III. SPHERICAL POINT SAMPLING

Three types of 3D laser devices are commonly employed to obtain range data:

- Commercial short range 3D devices with reduced field of view, usually applied for reversed engineering or generating computer graphics of small objects [11] [10] [12].
- High-end long range 3D devices with high resolution employed for realistic visualization and documentation of sites of interest [2] [16].
- Standard 2D devices with an extra degree freedom used for scene registration. This solution is commonly adopted in mobile robotics [1] [17] and also in the experiments that illustrate this paper.

Most of them perform a 2D scan in combination with a rotation of the opto-mechanical head, i.e. a spherical scan [16]. This is illustrated in Fig. 1 by a standard 180° 2D scanner with an additional degree of freedom at the sensor X axis. The paper focuses only on this case, but the proposed method can be adapted easily to rotation about the Y axis.

Dots in Fig. 1 do not represent ranges but measurement directions with respect to the origin of the scanner coordinate system. Thus, the resulting lune corresponds to the field of view of the sensor, which is defined by the maximum scanning angles of spherical coordinates: Φ for the 2D device and Ψ for the additional rotation. Besides, dot density in the lune illustrates angular resolution, which is given by $\Delta\phi$ and $\Delta\psi$, respectively. Thus, a 3D scan consists of N_ψ 2D slices composed of N_ϕ laser readings each:

$$N_\psi = 1 + \frac{\Psi}{\Delta\psi}; \quad N_\phi = 1 + \frac{\Phi}{\Delta\phi} \quad (1)$$

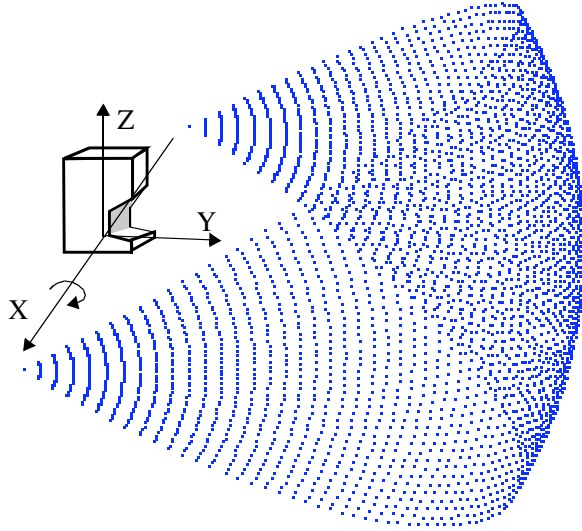


Fig. 1. Field of view and measure-direction density.

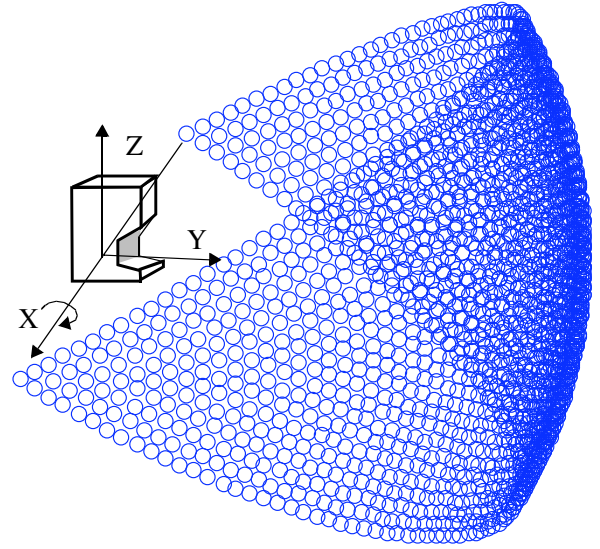


Fig. 2. Spherical point sampling.

The resulting number of raw data is given by $N = N_\psi \cdot N_\phi$. These can be represented as a range matrix R , where the element $r_{i,j}$ is the j -th data from the i -th 2D scan.

Because of this type of mechanism, maximum measure-direction density is located near the rotation axis [17]. The proposed sampling method takes into account this fact to equalize measure-direction densities, i.e. to discard readings that correspond to similar directions.

Note that for $\Psi = 180^\circ$, the first and the last scan directions coincide for all 2D slices (i.e., lune vertices in Fig. 1). This means that the ranges of the first and the last columns of matrix R would be similar in a static environment, so only one value for each column is necessary.

Scan densities get sparser when the direction approaches the YZ plane (i.e., in the forward direction of the sensor), so the central value of all N_ψ slices should be kept in the central column. Thus, the central column can be used as a reference to equalize the rest of the columns j proportionally to their normalized vertical arc lengths a_j :

$$a_j = \sin\left(\frac{\pi - \Phi}{2} + \Delta\phi(j - 1)\right) \quad (2)$$

where $\Phi \leq \pi$.

Thus, the number of row points selected for every column j in R is computed as:

$$s_j = \text{round}(1 + (N_\psi - 1) \cdot a_j) \quad (3)$$

Then, uniformly distributed row indexes to be kept for every j th column in R are obtained as vector I_j :

$$I_j = \left[1 + \text{round}\left(\left(\frac{N_\psi - 1}{s_j - 1}\right)(k - 1)\right) \right]_{k=1..s_j} \quad (4)$$

The result of applying this spherical sampling method can be observed in Fig. 2, where selected range directions appear as 'o's. The selected points in R make up a binary

mask matrix M that only has to be computed once for a particular scanner configuration. Then, element-by-element multiplication of M with R will systematically produce sampling for each scan.

The total proportion of sampled points from the original 3D scan can be computed as:

$$r_s = \sum_{j=1}^{N_\phi} \frac{s_j}{N} \quad (5)$$

which only depends on Φ and is independent of the angular resolution of the sensor. For instance, $r_s = 63.7\%$ for the case of $\Phi = 180^\circ$, which is the usual case for scene registration. This rate enlarges if the horizontal scope Φ is narrower (e.g., $r_s = 72.8\%$ for $\Phi = 150^\circ$).

IV. APPLICATION TO 3D SCENE GENETIC REGISTRATION

A. 3D Scanner Device

The 3D scanner device (see Fig. 3) has been constructed by adding an extra degree of freedom to a commercial 2D SICK-LMS 291 time-of-flight rangefinder.

The maximum values for the rangefinder specifications are: field of view $\Phi = 180^\circ$, horizontal angular resolution $\Delta\phi = \frac{1}{2}^\circ$, up to 80 m range, ± 4 cm range error, 26 ms of scan time and a serial interface at 500 Kbaud.

This 2D sensor has been incorporated into a mechanical articulation driven by a stepper motor. Its rotation axis has been made to coincide with the rangefinder's X axis through an eccentric gear. This way, readings are provided directly in spherical coordinates. Moreover, a special counterweight has been added to reduce the required driving torque.

The vertical angular resolution is $\Delta\psi = \frac{1}{3}^\circ$, with $\Psi = 60^\circ$ of field of view. A complete 3D scan with $N = 65341$ (361 · 181) points is obtained in a 12 s interval. The 2D rangefinder is continually sending range data with a refresh



Fig. 3. The 3D laser scanner is based on a 2D rangefinder.

rate that is faster than drive control. Synchronization is achieved by waiting for the step acknowledgement from the drive controller. At that time, the next complete 2D scan is recorded through the serial interface and, then, a new motion pulse is issued.

B. Spherical Point Sampling

Figures 4 to 6 show the mask matrix M obtained for different systematic approaches, where discarded points are shown in black. Figs. 4 and 5 illustrate uniform and random sampling, respectively, with a total sampling rate $r_s = 63.7\%$. The same number of points is selected in Fig. 6 by the spherical sampling algorithm. However, these are equalized according to measure direction density with respect to the maximum vertical resolution provided by the sensor.

C. Indoor Scene

Tests have been performed in a non-structured scene, provided by a cluttered robotics laboratory. Fig. 7 is a panoramic view of this scene composed by several stitched photographs. The same scene is depicted in Fig. 8 as the range matrix R recorded by the laser scanner. In this representation of 3D data, closer objects have a darker level of grey. White points correspond either to very far ranges or to invalid laser data.

This depth image resembles the panoramic view. Note that straight lines are distorted in a spherical way around the laser center. However, this image is more compact and intuitive for scenes than rendering virtual views only with this laser data.

Fig. 9 shows another view of the robotics laboratory. In particular, $x = -1\text{cm}$, $y = 39\text{cm}$, $z = 4\text{cm}$ and

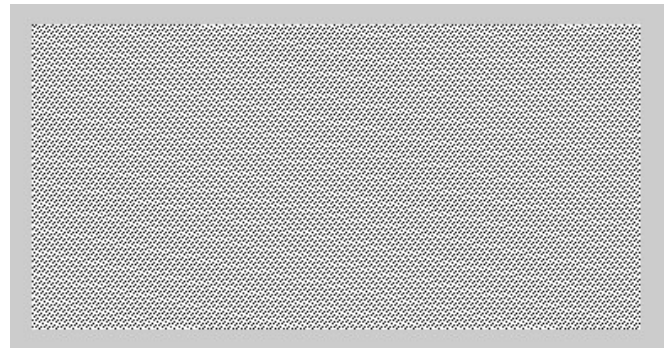


Fig. 4. Binary mask for uniform sampling.

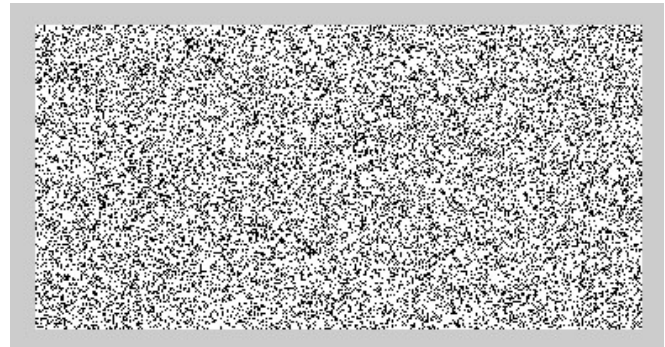


Fig. 5. Binary mask for random sampling.

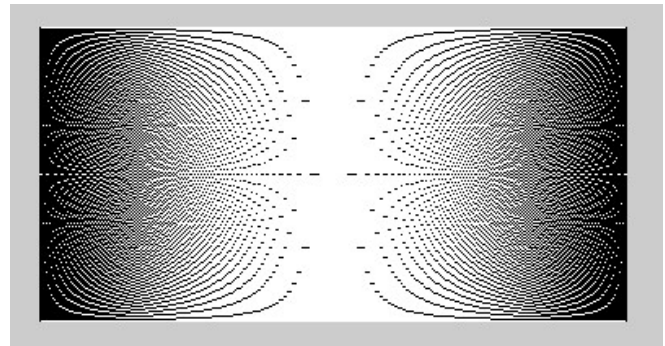


Fig. 6. Binary mask for spherical sampling.

$\alpha = -44.5^\circ$, $\beta = -0.8^\circ$, $\gamma = 9.1^\circ$ with respect to the reference coordinate system of the previous scan. The result of projecting this scan according to this transformation is shown in Fig. 10. White areas corresponds with no overlapping zones between both views.

D. Genetic Algorithm Registration

Regarding the GA registration method, pose-based encoding has been adopted (displacements x, y, z and angles α, β, γ with roll-pitch-yaw convection). Sampling is applied only to the projected scan.

Range differences of the same measure direction between the projected and reference scans have been considered for the fitness function. A threshold of 10 cm for the difference



Fig. 7. Panoramic view of the laboratory with the mobile robot Auriga- α centered on the foreground.



Fig. 8. Depth image of the robotics laboratory (reference scan).



Fig. 9. Second view of the robotics laboratory (scan to be projected).



Fig. 10. Optimal projection of the second scan into the reference coordinate system.

between the actual and projected ranges is used to reject non-matched ranges for the fitness function [9].

Each gene has been coded into a 6-bit string, thus forming individuals of 36 bits. The boundaries of the problem space around the initial estimation are defined by maximum errors of ± 8 cm for displacements and of $\pm 4^\circ$ for rotations.

The GA has been set to iterate 120 generations with a population size of 80 solutions. The individuals above the fitness arithmetic mean are replaced every generation. One-point crossover is applied to the parents, which are chosen randomly from the entire population. The mutation rate has been set to 1 bit per 2 new chromosomes.

E. Experimental results

Fig. 11 shows the relationship between the number of points projected into the reference scan (logarithmic scale) and the processing time of GA implemented as described in previous subsection. Computations have been carried out by a PC with Pentium IV at 3.2GHz. The processing time is

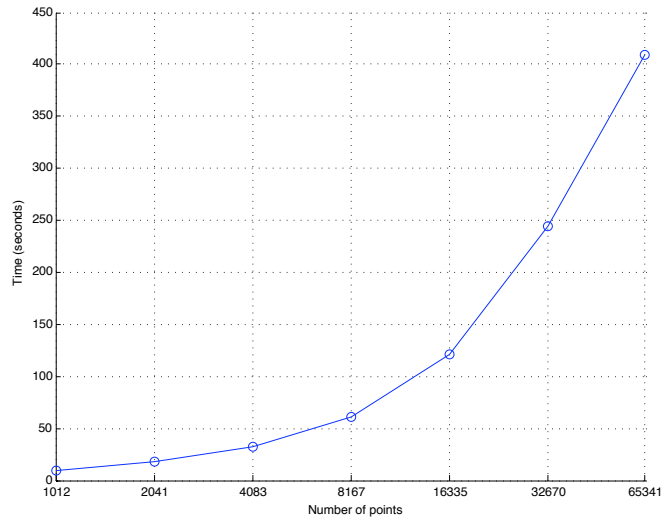


Fig. 11. Relationship between number of points and processing time.

TABLE I
EXPERIMENTAL SCAN MATCHING ERRORS.

| Sampling | Points | E_s (cm) | E_a ($^\circ$) | Matches |
|------------|--------|------------|--------------------|---------|
| All points | 65341 | 0.64 | 0.25 | 34291 |
| Random | 41619 | 0.58 | 0.29 | 21738 |
| Uniform | 41619 | 0.54 | 0.33 | 21632 |
| Spherical | 41619 | 0.86 | 0.22 | 23179 |

linear with the number of points and is almost independent of the number of matched points due to the pose-based encoding.

Table I summarizes a set of GA registrations of the scans presented in subsection IV-C. For each systematic sampling method, ten matchings have been averaged with different initial pose estimations.

Two accuracy measures are shown in table I. Let $\Delta x, \Delta y, \Delta z, \Delta \alpha, \Delta \beta, \Delta \gamma$ be the errors between the estimated pose and the ground truth. Then, E_s represents the euclidean distance: $\sqrt{\Delta x^2 + \Delta y^2 + \Delta z^2}$, and E_a represent the angular error of the three rotations: $\sqrt{\Delta \alpha^2 + \Delta \beta^2 + \Delta \gamma^2}$.

As can be observed, GA registration method is quite robust because the errors are close to the resolution of the search space. Moreover, the effect of the sampling methods is almost negligible, being spherical, the technique with the bigger proportion of matched points.

V. CONCLUSIONS

Present-day 3D scanners offer high point density, but certain applications of scene registration, like mobile robotics, impose time constraints. Thus, point sampling plays an important role both on the accuracy of the resulting pose estimation and on computational requirements.

We propose a new point samplig method that considers the spherical scanning process of most laser sensors in order to equalize the measure-direction density. The major advantages of this approach are:

- It does not depend on actual range readings, so its computational load is similar to that of random or uniform sampling. A binary mask, that is computed once for a given sensor configuration, is used to systematically select data from each scan.
- It can achieve up to 36.3% of data reduction while preserving the angular resolution of the original sensor, so it is less likely that relevant scene information is lost.
- Equalization not only produces sampling, but also avoids that denser peripheral regions of the scene have more weight in the matching process.

Spherical sampling has been successfully applied to 3D scene registration, a problem with special difficulties as compared to 2D or single-object matching. We find that GA's provide a robust search which a computational load proportional to the number of sampled data.

In the case that maintaining the original resolution of sensor data is not a major aim, the concept of equalization measure-direction density could be extended to increase data reduction.

Further comparisons are required with faster but less reliable registration algorithms as well as with range dependent sampling methods. Another extension of this work includes its application to mobile robot mapping in outdoor areas.

ACKNOWLEDGMENTS

This work was partially supported by the Spanish CICYT projects DPI 2005-01391 and DPI 2005-00207. We thank A. Pequeño-Boyer for constructing the 3D laser device.

REFERENCES

- [1] A. Nüchter, H. Surmann, K. Lingemann, J. Hertzberg, and S. Thrun, "6D SLAM with an application in autonomous mine mapping," in *Proc. IEEE International Conference on Robotics & Automation*, New Orleans, 2004, pp. 1998–2003.
- [2] P. Allen, I. Stamos, A. Gueorguiev, E. Gold, and P. Blaer, "AVENUE: Automated site modelling in urban environments," in *Proc. IEEE 3 Digital Imaging and Modelling*, Canada, 2001, pp. 357–364.
- [3] P. J. Besl and N. D. McKay, "A method for registration of 3D shapes," *IEEE Transactions on Pattern Analysis and Machine Intelligence*, vol. 14, pp. 239–256, 1992.
- [4] Z. Zhang, "Iterative point matching for registration of free-form curves," INRIA, France, Technical Report 1658, 1992.
- [5] S. Rusinkiewicz and M. Levoy, "Efficient variants of the ICP algorithm," in *Proc. 3th Int. Conf. on 3D Digital Imaging and Modelling*, Canada, 2001, pp. 145–152.
- [6] P. J. Neugebauer, "Geometrical cloning of 3D objects via simultaneous registration of multiple range images," in *Proc. IEEE Int. Conf. on Shape Modeling and Applications*, Japan, 1997, pp. 130–139.
- [7] G. Blais and M. D. Levine, "Registering multiview range data to create 3D computer objects," *IEEE Transactions on Pattern Analysis and Machine Intelligence*, vol. 17, pp. 820–824, 1995.
- [8] A. Agrawal, N. Ansari, and E. S. H. Hou, "Evolutionary programming for fast and robust point pattern matching," in *Proc. IEEE/RSJ International Conference on Intelligent Robots and Systems*, Germany, 1994, pp. 1777–1782.
- [9] J. L. Martínez, J. González, J. Morales, A. Mandow, and A. J. García-Cerezo, "Mobile robot motion estimation by 2D scan matching with genetic and iterative closest point algorithms," *Journal of Field Robotics*, vol. 23, pp. 21–34, 2006.
- [10] L. Silva, O. R. P. Bellon, K. W. Jörg, and K. L. Boyer, "Precision range image registration using a robust surface interpenetration measure and enhanced genetic algorithms," *IEEE Transactions on Pattern Analysis and Machine Intelligence*, vol. 27, pp. 762–776, 2005.
- [11] K. Brunnstrom and A. J. Stoddart, "Genetic algorithms for free-form surface matching," in *Proc. 13th International Conference on Pattern Recognition*, vol. 4, Austria, 1996, pp. 689–693.
- [12] J. W. Branch, F. Prieto, and P. Boulanger, "Correspondence method for registration of range images using evolutionary algorithms," in *Proc. IEEE International Conference on Industrial Electronics and Control Applications*, Ecuador, 2005, pp. 1–6.
- [13] G. Turk and M. Levoy, "Zippered polygon meshes from range images," in *Proc. of the 21th Conference on Computer Graphics and Interactive Techniques*, Orlando, 1994, pp. 311–318.
- [14] S. Weik, "Registration of 3D partial surface models using luminance and depth information," in *Proc. IEEE 3 Digital Imaging and Modelling*, Canada, 1997, pp. 93–100.
- [15] C. Robertson and R. B. Fisher, "Parallel evolutionary registration of range data," *Computer Vision and Image Understanding*, vol. 87, pp. 39–50, 2002.
- [16] A. Wehr, "Laser scanning and its potential to support 3d panoramic recording," in *Proc. ISPRS Workshop on Panoramic Photogrammetry*, Germany, 2005.
- [17] J. L. Martínez, A. Pequeño-Boyer, A. Mandow, A. García-Cerezo, and J. Morales, "Progress in mini-helicopter tracking with a 3D laser range-finder," in *Proc. 16th IFAC World Congress*, Czech Republic, 2005.